

Photonic Controlled-Phase Gates Through Rydberg Blockade in Optical Cavities

Sumanta Das^{1,*}, Andrey Grankin^{2,†}, Ivan Iakoupov¹, Etienne Brion³, Johannes Borregaard^{1,4}, Rajiv Boddeda², Imam Usmani², Alexei Ourjoutsev², Philippe Grangier², and Anders S. Sørensen¹

¹ *The Niels Bohr Institute, University of Copenhagen, Blegdamsvej 17, DK-2100 Copenhagen Ø, Denmark*

² *Laboratoire Charles Fabry, Institut d'Optique, CNRS, Univ Paris-Sud, Campus Polytechnique, RD 128, 91127 Palaiseau cedex, France*

³ *Laboratoire Aimé Cotton, CNRS, Université Paris Sud, ENS Cachan, 91405 Orsay, France.*

⁴ *Department of Physics, Harvard University, Cambridge, MA 02138, USA*

(Dated: September 16, 2015)

We propose a novel scheme for high fidelity photonic controlled-phase gates using Rydberg blockade in an ensemble of atoms in an optical cavity. The gate operation is obtained by first storing a photonic pulse in the ensemble and then scattering a second pulse from the cavity, resulting in a phase change depending on whether the first pulse contained a single photon. We show that the combination of Rydberg blockade and optical cavities effectively enhances the optical non-linearity created by the strong Rydberg interaction and makes the gate operation more robust. The resulting gate can be implemented with cavities of moderate finesse allowing for highly efficient processing of quantum information encoded in photons. As an illustration, we show how the gate can be employed to increase the communication rate of quantum repeaters based on atomic ensembles.

PACS numbers:

Keywords:

Large bandwidth, fast propagation and the non-interacting nature of photons, make them ideal for communicating quantum information over long distances [1]. In contrast, strong photon-photon interactions are desirable for processing of quantum information encoded in the photons, especially if both high fidelity and high efficiency are needed. To satisfy these requirements one needs a highly non-linear medium. Typically, the strength of photon-photon interactions mediated by a non-linear medium is very weak at the single-photon level where photonic quantum logic gates are operating [2]. As a consequence, the implementation of photonic quantum gates remains an unsolved challenge and requires novel means of efficient light-matter interaction. To enhance light-matter interactions, a viable solution is to use ensembles of atoms, e.g., configured for electromagnetically induced transparency (EIT) [3]; this can be further improved by placing the ensemble in an optical cavity, but these ensemble based approaches do not increase the essential photonic non-linearity. In recent years, there has been intense efforts to realize light-matter interactions via, non-linear interactions in a variety of medium, ranging from atoms [4–10] and atom like systems [11–14] to superconducting qubits [15–17].

A promising approach towards creating strong quantum nonlinearities is to exploit excitation blockade in Rydberg EIT systems [18–25]. Several quantum effects like strong optical non-linearities and control of light by light [22–28], deterministic single-photon sources [29], and the generation of entanglement and atomic quantum gates [30–34] have been investigated. The strong nonlinearity originates from the fact that the Rydberg interaction prevents multiple excitations within a blockaded radius r_b [35, 36]. The ensemble then behaves as a two-level *superatom* consisting of N_b atoms within a radius r_b [35, 36]. If the optical depth d_b corresponding to the superatom is sufficiently large, $d_b \gg 1$ [22], a strong optical nonlinearity at the single-photon level can be achieved in the EIT configuration [18–25]. Reaching such an optical depth is,

however, challenging, which limits the effectiveness of photonic quantum gates.

An enhanced optical nonlinearity was recently demonstrated by placing the ensemble inside an optical cavity [26], but a direct application of this nonlinearity for quantum gates is non-trivial since the outgoing optical modes are highly distorted and entangled by the interaction [37–39]. In this letter, we propose a novel scheme for achieving a high fidelity *photonic controlled-phase (CP) gate with a Rydberg EIT ensemble* trapped inside an optical cavity of moderate finesse. In our scheme, the photons are incident at different times thus avoiding the problem of mode distortion while still allowing the cavity enhancement of the interaction. The use of a cavity has several major advantages compared to ensembles in free space, since it enhanced light-atom coupling in the ensemble and also effectively increases the non-linearity. In our proposal, the parameter characterizing the Rydberg blockade is $C_b \sim \mathcal{F}d_b$, where $C_b = N_b\mathcal{C}$, with $\mathcal{C} \ll 1$ being the single atom cooperativity, and \mathcal{F} is the cavity finesse. Hence the effect of the Rydberg interaction is increased by the cavity finesse \mathcal{F} , whereas the low value of \mathcal{C} is compensated by a high value of N_b . In addition, the cavity is also useful for controlling the mode structure thereby enabling high input-output efficiencies [40]. We show that the proposed gate can have a promising (heralded) error scaling as $1/C_b^2$, and demonstrate how it can be used to improve quantum repeaters based on atomic ensembles even for moderate interaction strengths $C_b \sim 10$. The proposed CP gate can thus be directly integrated into quantum communication circuitry thereby providing a building block for future quantum networks. The Rydberg interaction [36] for our proposal can either be long range dipolar or van der Waals interactions, but for simplicity, we only consider the latter.

We first outline the basic idea of our gate, which goes along the line of Ref. [41], except that the single trapped atom is replaced by a Rydberg ensemble. In contrast to Ref. [41],

and many others, we thus do *not* require the strong-coupling regime of cavity QED, and can work with cavities of moderate finesse. This enables input-output efficiency near unity since the cavity losses can be completely negligible compared to the mirror's transmission [40]. For simplicity, we first describe the operation for single-rail qubits where a qubit is encoded in a photon pulse containing a superposition of vacuum $|0\rangle$ and a single photon $|1\rangle$. Later, we generalize it to a more useful dual-rail encoding where the qubit is encoded as a photon in one of two possible modes.

In the single-rail version outlined in Figs. 1(a) and (b), a first photon pulse is stored in a cavity containing a Rydberg EIT ensemble [42]. Here a classical driving field from an excited state $|e\rangle$ to a Rydberg state $|r\rangle$ enables the storage of incoming photons in $|r\rangle$ through the interaction of the cavity field with the transition from the ground state $|g\rangle$ to $|e\rangle$. The excitation in state $|r\rangle$ is then transferred to another Rydberg state $|r'\rangle$ by a microwave pulse so that the ensemble contains a single atom in state $|r'\rangle$ if the first pulse contained a single incoming photon. The second pulse is then incident on the cavity. If the first pulse contained vacuum $|\emptyset\rangle$, the second pulse is scattered under Rydberg EIT conditions and leaves the cavity with the same phase. If the first pulse contained a photon, the atom in $|r'\rangle$ shifts the position of the state $|r\rangle$ in the remaining atoms. As we will show, this prevents the second pulse from entering the cavity resulting in a phase flip on the $|1\rangle$ component of the second pulse. This evolution thus realizes a CP gate which, together with single qubit operations, is universal for quantum information processing.

We now present a theoretical treatment to evaluate the performance of the CP gate. The initial state of the single photon pulse can be expressed as $\int d\omega \phi(\omega) \hat{a}_\omega^\dagger e^{-i\omega t} |\emptyset\rangle$, where $\phi(\omega)$ is the normalized pulse shape, \hat{a}_ω^\dagger is the one-dimensional field operators satisfying the standard bosonic commutation relations and $|\emptyset\rangle$ denotes the vacuum of all the optical modes. The frequency integrand ω of the incoming photon is referenced to the cavity frequency ω_c , which in turn is nearly resonant to the $|e\rangle \rightarrow |g\rangle$ transition (see Fig. 1(a)). The cavity is assumed to be one-sided with a standing-wave field. The dynamics of the system can be described in the quantum jump approach through the no-jump Hamiltonian $\mathcal{H} = \mathcal{H}_s + \mathcal{H}_I$. Here \mathcal{H}_s consists of the decays and the free energy terms [43] while,

$$\begin{aligned} \mathcal{H}_I = & - \sum_l \hbar \left[\frac{\Omega_l}{2} |r_l\rangle \langle e_l| + i\mathcal{G}_l |e_l\rangle \langle g_l| \hat{b} \right] + \text{H.c.} \\ & + \sum_k \hbar \mathcal{V}_{kl} |r'_k\rangle \langle r'_k| \otimes |r_l\rangle \langle r_l|, \end{aligned} \quad (1)$$

Here the coupling strengths of the l^{th} atom with the driving field and the incoming single photon pulse is respectively Ω_l and \mathcal{G}_l , while \mathcal{V}_{kl} is the van der Waals interaction among the Rydberg excitations of atoms k and l . We solve the Schrödinger equation for the scattering stage assuming constant Ω_l in Fourier space to find the reflection co-efficient. The (amplitude) reflection coefficient with the stored Rydberg excitation in atom k is given by $\mathcal{R}_k(\omega) = (2\kappa \mathbf{S}_k(\omega) - 1)$

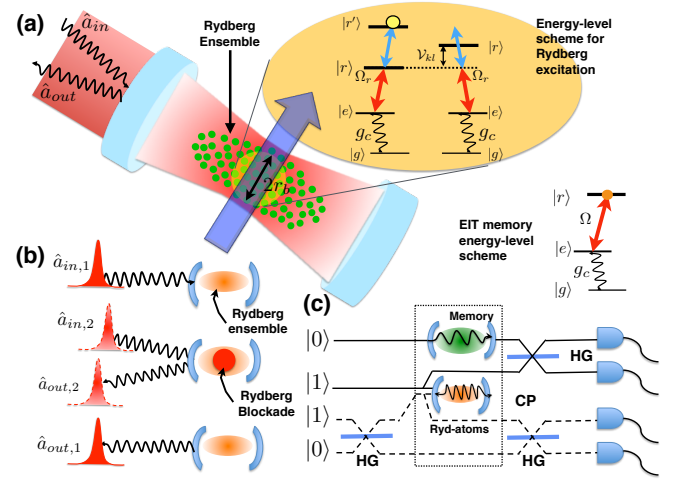


FIG. 1: Schematic outline of the phase gate (a) An input single photon pulse along with a driving field induces a two-photon transition to the Rydberg state $|r\rangle$ which is subsequently transferred to another Rydberg state $|r'\rangle$. Due to Rydberg interactions \mathcal{V}_{kl} among the atoms, other Rydberg states $|r\rangle$ within the range of the interaction potential, given by, the blockade radius of r_b , become off-resonant allowing no further excitation. (b) When an initial photon pulse is stored in the Rydberg ensemble, the second incoming photon cannot enter the cavity and is scattered off, which ideally induces a phase flip of π on the scattered photons. (c) Dual-rail implementation of a CP gate (dotted box). A Bell state measurement can be implemented by combining the CP gate with Hadamard gates (HG).

where,

$$\mathbf{S}_k(\omega) = \left(\kappa - i\omega + \sum_l \frac{|\mathcal{G}_l|^2}{(\Gamma_{el} - i\tilde{\Delta}_l) + \frac{|\Omega_l/2|^2}{\Gamma_{rl} + i(\delta_l + \mathcal{V}_{kl} - \omega)}} \right)^{-1}. \quad (2)$$

where the detunings are $\Delta_l = \omega_{e_l} - \omega_c$, $\tilde{\Delta}_l = \Delta_l + \omega$ and $\delta_l = (\omega_{r_l} - \omega_e) - \omega_c$ with $\hbar\omega_{e_l(r_l)}$ and $\Gamma_{e_l(r_l)}$ being the energy and width of the excited (Rydberg) state $|e\rangle(|r\rangle)$ in atom l and κ is the cavity field decay rate. The reflection coefficient $\mathcal{R}_g(\omega)$ [43] for no stored excitation is evaluated by setting $\mathcal{V}_{kl} = 0$.

To get an understanding of the scattering we study the behavior of the reflection coefficient for resonant interactions $\delta_l = \Delta_l = 0$ and long lived Rydberg excitations ($\Gamma_{rl} = 0$). For simplicity, we assume equal couplings and driving strengths on all atoms $\mathcal{G}_l = \mathcal{G}$ and $\Omega_l = \Omega$ (for the general case see [43]). Furthermore, if the photon pulse has a suitably long duration we can put $\omega \approx 0$ (see below). With these assumptions, we find from Eq. (S14) that $\mathcal{R}_g = 1$ for no stored excitation; this is the perfect EIT condition. When an excitation is stored, the reflection coefficient becomes

$$\mathcal{R}_k = \left(\frac{2}{1 + \mathcal{C}_v^*} - 1 \right), \quad (3)$$

where $\mathcal{C}_v^* = \mathcal{C}_b + i\mathcal{C}'_b = \mathcal{C} \sum_l 1 / \left[1 + \frac{|\Omega/2|^4}{\mathcal{V}_{kl}^2 \Gamma_e^2} \right] + i\mathcal{C} \sum_l \frac{|\Omega/2|^2}{\mathcal{V}_{kl} \Gamma_e} \left[1 + \frac{|\Omega/2|^4}{\mathcal{V}_{kl}^2 \Gamma_e^2} \right]$ quantifies the effective coopera-

tivity of the blockade, while $\mathcal{C} = |\mathcal{G}|^2/(\kappa\Gamma_e)$ is the single atom cooperativity. Each atom l in the volume blocked by the $|r'_k\rangle$ excitation, *i.e.* such that $\mathcal{V}_{kl} \gg |\Omega/2|^2/\Gamma_e$, will contribute with \mathcal{C} in \mathcal{C}_b . On the other hand, those atoms for which $\mathcal{V}_{kl} \ll |\Omega/2|^2/\Gamma_e$ will have a negligible contribution to \mathcal{C}_b , and hence \mathcal{C}_b gives the effective cooperativity of the blockade ensemble. The imaginary part depends on the shape of the interaction but for a uniform $1/r^6$ interaction at resonance in a uniform cloud we find that $|\mathcal{C}'_b| = \mathcal{C}_b$ [43] (r is the distance between atoms k and l).

We now discuss the key feature of our work - the implementation of a photonic CP gate via scattering from a Rydberg ensemble in either a single-rail or dual-rail encoding. The single-rail implementation uses the encoding discussed in the introduction and is shown schematically in Fig. 1 (b). A first qubit is encoded in the vacuum and single photon state, $|\mathcal{O}\rangle$ and $|1\rangle = \int d\omega \phi(\omega) \hat{a}_\omega^\dagger e^{-i\omega t} |\mathcal{O}\rangle$, respectively, of a first incoming pulse. This pulse is stored in the Rydberg ensemble such that the logical states $|0\rangle$ and $|1\rangle$ are mapped onto the ensemble being in the joint ground state $|0\rangle = |g^N\rangle |\mathcal{O}\rangle$ and a Rydberg polariton $|1\rangle = \sum_k \alpha_k |g^{N-1}, r'_k\rangle |\mathcal{O}\rangle$. This is achieved using the well established techniques of storage in atomic ensembles, which is known to have an error $1/N\mathcal{C}$ for any slowly varying pulse shape provided a temporally varying control field is used during storage [3, 19], followed by microwave π -pulse between $|r_k\rangle$ and $|r'_k\rangle$. A second incoming photon pulse is then reflected from the cavity. This reflection can be from either an ensemble in the EIT configuration (ensemble in $|0\rangle$), or from a blocked ensemble ($|1\rangle$). As can be seen from Eq. (S17) there is exactly a π phase shift between the two situations: $\mathcal{R}_g = 1$ for $\mathcal{C}_v^* = 0$ and $\mathcal{R}_k = -1$ for $|\mathcal{C}_v^*| \gg 1$. Finally, the first stored pulse is retrieved from the ensemble.

To evaluate the performance we calculate the Choi-Jamiolkowski fidelity of the gate. Since, in general, we have $N\mathcal{C} > \mathcal{C}_b$, the fidelity of the operation will mainly be limited by the gate and we shall ignore imperfections during the storage. The fidelity can then be determined by [43],

$$F_{\text{CJ}} = \frac{1}{16} \left| 2 + \int d\omega |\phi(\omega)|^2 \mathcal{R}_g(\omega) - \sum_k \int d\omega |\alpha_k|^2 |\phi(\omega)|^2 \mathcal{R}_k(\omega) \right|^2. \quad (4)$$

To account for errors due to imperfect Rydberg blockade, we evaluate the above fidelity and find

$$F_{\text{CJ}} = 1 - \frac{(1 + \mathcal{C}_b)}{(1 + \mathcal{C}_b)^2 + \mathcal{C}_b'^2} - \frac{N\mathcal{C}\Gamma_e^2}{|\Omega/2|^4} (\Delta\omega)^2 - \left(\frac{1}{\kappa} + \frac{N\mathcal{C}\Gamma_e}{|\Omega/2|^2} \right)^2 (\Delta\omega)^2 \quad (5)$$

Here the third and fourth term are gate errors due to the finite frequency width $\Delta\omega^2$ of the incoming pulse. These terms arise predominately from the EIT bandwidth, which is much narrower than the variations of the blocked reflection coefficient. For a narrow pulse $\Delta\omega \rightarrow 0$, the fidelity is only limited

by the cooperativity of the blocked ensemble $1 - F_{\text{CJ}} \propto 1/\mathcal{C}_b$. Hence, as discussed in the introduction, it is the cavity enhanced blocked cooperativity, which is the main figure of merit for the gate.

In the dual-rail encoding, both logical states $|0\rangle$ and $|1\rangle$ are represented by photons, but in two different paths. A schematic of the dual-rail CP gate is shown in Fig. 1(c). The first photon pulse in the upper two arms of the figure is first stored in a memory consisting of a Rydberg ensemble placed in each arm (for a polarization encoding such two memories might be realized by two different internal states of the same ensemble). A second photon pulse is then scattered from the Rydberg ensemble if it is in state $|1\rangle$ (upper rail in the figure). This scattering ideally induces a phase change of π if there was a photon stored in the Rydberg ensemble, *i.e.* if both qubits were in state $|1\rangle$. As opposed to the single-rail implementation, the dual-rail implementation has the possibility of conditioning on getting two photons in the output. Since the dominant error in the single-rail implementation is the loss of photons, this possibility allows for a substantial increase in the fidelity with only a minor failure probability of the gate. In view of a possible application of the gate for quantum repeaters, discussed below, we consider the conditional fidelity of an EPR pair resulting from an entanglement swap realized with the gate using the full circuit in Fig. 1(c). Neglecting again the error due to finite storage efficiency, we find that this fidelity is [43]

$$F_{\text{swap}} = \frac{\int d\omega |\phi(\omega)|^2 |2 + \mathcal{R}_g(\omega) - \sum_k |c_k|^2 \mathcal{R}_k(\omega)|^2}{16P_{\text{suc}}} \quad (6)$$

where the success probability of the process is $P_{\text{suc}} = \int d\omega |\phi(\omega)|^2 (2 + |\mathcal{R}_g(\omega)|^2 + |\sum_k |c_k|^2 \mathcal{R}_k(\omega)|^2)/4$. Note that compared to F_{CJ} in Eq. (S19), the only difference is due to the conditioning with a success probability $P_{\text{suc}} < 1$ and the way the mode function is treated. The latter is related to the fact that Eq. (S19) is the fidelity with a specific mode function. Keeping only the leading order contribution to the dispersion, we find the fidelity and success probability of the CP gate

$$F_{\text{swap}} = 1 - \frac{1}{[\mathcal{C}_b^2 + \mathcal{C}_b'^2]} - \frac{3\mathcal{C}_b^2 - \mathcal{C}_b'^2}{4[\mathcal{C}_b^2 + \mathcal{C}_b'^2]^2} - \frac{3}{4} \left[\frac{1}{\kappa} + \frac{N\mathcal{C}\Gamma_e}{|\Omega/2|^2} \right]^2 (\Delta\omega)^2, \quad (7)$$

$$P_{\text{suc}} = 1 - \frac{\mathcal{C}_b}{(1 + \mathcal{C}_b)^2 + \mathcal{C}_b'^2} - \frac{N\mathcal{C}\Gamma_e^2}{|\Omega/2|^4} (\Delta\omega)^2 \quad (8)$$

Here the fourth term is again the leading order error from the spectral width of the pulse. In the limit of a narrow pulse $\Delta\omega \rightarrow 0$, we see that the conditional gate error $1 - F_{\text{swap}} \propto 1/(\mathcal{C}_b)^2$ for $\mathcal{C}_b \gg 1$ is much smaller than for the single-rail. This comes at only a minor cost in the failure probability $1 - P_{\text{suc}} \propto 1/\mathcal{C}_b$. The resulting dual-rail fidelities are plotted in Fig. 2 as a function of the parameter \mathcal{C}_b . For $\mathcal{C}_b \approx 8$, the (post-selected) fidelity is found to be larger than 0.99

In order to get realistic predictions, we use the experimental conditions of Ref. [26], with $\Gamma_e \approx (2\pi)3\text{MHz}$ and

$\kappa \approx (2\pi)10\text{MHz}$ (corresponding to a finesse $\mathcal{F} \approx 120$) but a smaller beam waist $w_0 = 15\mu\text{m}$. This gives a single atom cooperativity $\mathcal{C} = 0.025$ and we take $N\mathcal{C} = 20$ corresponding to a combined storage and retrieval efficiency of 90%. We assume a Rydberg line width $\gamma_r = (2\pi)60\text{kHz}$ [44] corresponding to a coherence time of $\tau_r = 1/\gamma_r = 2.65\mu\text{s}$ (note that if the two ensembles in the dual-rail encoding are read out with the same laser the scheme becomes insensitive to phase fluctuations). With a pulse duration of $T = 1/\Delta\omega = 300\text{ns}$ and a driving strength of $\Omega = (2\pi)36\text{MHz}$ the error due to finite bandwidth in Eq. (S22) is below 2%. Taking the interaction $\mathcal{V} = (2\pi)8.31 \cdot 10^6/r^6\text{MHz}\mu\text{m}^6$ corresponding to two atoms with a Rydberg quantum number $n_r = 90$ and an atomic density of $n = 0.25\mu\text{m}^{-3}$, one has $\mathcal{C}_b \sim 8.1$ [43] which is sufficient to obtain high fidelities as show in Fig. 2. Here, we ignore any effect of sample inhomogeneities, but this can be taken into account by suitable redefinitions of \mathcal{C}_b and \mathcal{C}'_b [43].

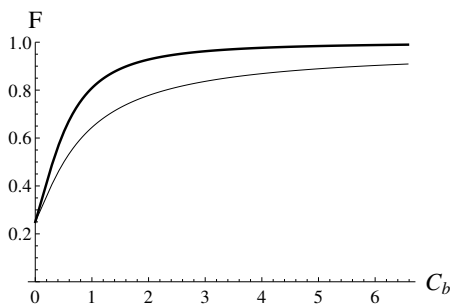


FIG. 2: Choi-Jamiolkowski fidelity (thin line) and post-selected swap fidelity (thick line) as functions of the blocked cooperativity \mathcal{C}_b for a spectrally narrow pulse $\Delta\omega \rightarrow 0$. We assume $|\mathcal{C}'_b| = \mathcal{C}_b$.

As a particular application of the gate, we consider long distance quantum cryptography based on quantum repeaters. We considered the ensemble based quantum repeater protocol proposed in Ref. [46], but replace the entanglement swapping with the procedure shown in Fig. 1(c). We calculate the secret key rate per repeater station as described in Ref. [45] (assuming the distributed states to be Werner states) and compare the results to the original protocol (see Fig. 3). At the lowest level of the protocol, single excitations are stored in atomic ensembles using a Raman scheme and we include double excitation errors to lowest order similar to Ref. [46]. The performance of the protocol depends strongly on the repetition rate of this operation. Regardless of the repetition rate, the CP gate enables significantly higher communication rates since it allows near perfect Bell state measurements (for $\mathcal{C}_b \gg 1$) whereas swapping operations based on linear optics have a maximal success probability of 50%. In Fig. 3, we also show the rate obtainable if single excitations are initially created perfectly and deterministically in the atomic ensembles, e.g., by exploiting Rydberg blockade [29]. We find that for such a protocol, a cooperativity of $\mathcal{C}_b \sim 25$ is sufficient to obtain a secret key rate of 1.5 Hz over 1000 km using 33 repeater stations.

In conclusion, we have proposed an efficient method to im-

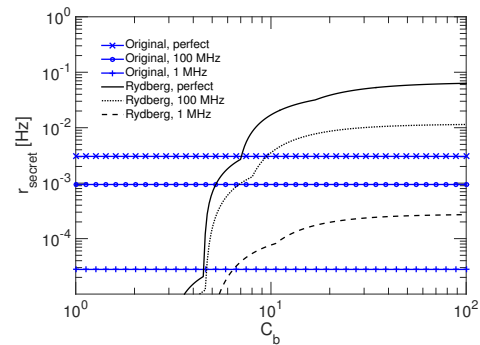


FIG. 3: Secret key rate per repeater station (r_{secret}) as a function of the blocked cooperativity (\mathcal{C}_b) for a communication distance of 1000 km. We compare the protocol of Ref. [46] (Original) with a modified protocol where the entanglement swapping is performed with the Rydberg CP gate (Rydberg). We consider an optimistic source repetition rate of 100 MHz and a more modest one of 1 MHz, as well as a perfect single excitation state created in the atomic ensembles, e.g., using Rydberg blockade [29]. We assume an attenuation length of 22 km in the fibers and an optical signal speed of $2 \cdot 10^5\text{ km/s}$. The ensemble readout efficiency and photodetector efficiency are both assumed to be 90%. The steps in the curves reflect where the fidelity of the CP gate allows additional swap levels to be employed.

plement a CP gate for photons. The gate combines the advantages of cavity defined optical modes and cavity enhanced light matter interactions with the strong Rydberg blockade obtainable in atomic ensembles. As a direct application, the proposed gate can be used to improve the communication rate of quantum repeaters, but more generally the gate may serve as a building block for photonic quantum networks.

The research leading to these results was funded by the European Union Seventh Framework Programme through SIQS (Grant No. 600645) and ERC Grant QIOS (Grant No. 306576). J.B. acknowledges funding from the Carlsberg foundation. S.D. and A.G. contributed equally to this work.

* Electronic address: sumanta@nbi.ku.dk

† Electronic address: andrey.grankin@u-psud.fr

- [1] H. J. Kimble, *Nature* **453**, 1023 (2008).
- [2] D. E. Chang, V. Vuletić and M. D. Lukin, *Nature Photonics* **8**, 685 (2014).
- [3] K. Hammerer, A. S. Sørensen, and E. S. Polzik, *Rev. Mod. Phys.* **82**, 1041 (2010).
- [4] Q. A. Turchette, C. J. Hood, W. Lange, H. Mabuchi, and H. J. Kimble, *Phys. Rev. Lett.* **75**, 4710 (1995).
- [5] S. E. Harris, and L. V. Hau, *Phys. Rev. Lett.* **82**, 4611 (1999).
- [6] B. Darquié, M. P. A. Jones, J. Dingjan, J. Beugnon, S. Bergamini, Y. Sortais, G. Messin, A. Browaeys, P. Grangier, *Science* **309**, 454 (2005).
- [7] M. K. Tey, Z. Chen, S. A. Aljunid, B. Chng, F. Huber, G. Maslennikov, and C. Kurtsiefer *Nature Phys.* **4**, 924 (2008).
- [8] W. Chen, K. M. Beck, R. Bücker, M. Gullans, M. D. Lukin, H. Tanji-Suzuki, and V. Vuletić, *Science* **341**, 768 (2013).
- [9] T. G. Tiecke, J. D. Thompson, N. de Leon, V. Vuletić, and M. D. Lukin, *Nature* **508**, 241 (2014).
- [10] A. Reiserer, N. Kalb, G. Rempe, and S. Ritter *Nature* **508**, 237

- (2014).
- [11] P. Michler, A. Kiraz, C. Becher, W. V. Schoenfeld, P. M. Petroff, Lidong Zhang, E. Hu, A. Imamoğlu, *Science* **290**, 2282 (2000).
- [12] I. Fushman, D. Englund, A. Faraon, N. Stoltz, P. Petroff, and J. Vučković, *Science* **320**, 769 (2008).
- [13] J. Hwang, M. Pototschnig, R. Lettow, G. Zumofen, A. Renn, S. Götzinger, and V. Sandoghdar *Nature* **460**, 76 (2009).
- [14] B. Casabone, K. Friebe, B. Brandstätter, K. Schüppert, R. Blatt, and T. E. Northup *Phys. Rev. Lett.* **114**, 023602 (2015).
- [15] M. H. Devoret and R. J. Schoelkopf, *Science* **339**, 1169 (2013).
- [16] P. Adhikari, M. Hafezi, and J. M. Taylor, *Phys. Rev. Lett.* **110**, 060503 (2013).
- [17] L. Neumeier, M. Leib, and M. J. Hartmann, *Phys. Rev. Lett.* **111**, 063601 (2013).
- [18] I. Friedler, D. Petrosyan, M. Fleischhauer, and G. Kurizki, *Phys. Rev. A* **72**, 043803 (2005).
- [19] A. V. Gorshkov, J. Otterbach, M. Fleischhauer, T. Pohl, and M. D. Lukin, *Phys. Rev. Lett.* **107**, 133602 (2011).
- [20] D. Petrosyan, J. Otterbach, and M. Fleischhauer, *Phys. Rev. Lett.* **107**, 213601 (2011).
- [21] J. Stanojevic, V. Parigi, E. Bimbard, A. Ourjoumtsev, and P. Grangier, *Phys. Rev. A* **88**, 053845 (2013).
- [22] J. D. Pritchard, D. Maxwell, A. Gauguet, K. J. Weatherill, M. P. A. Jones, and C. S. Adams, *Phys. Rev. Lett.* **105**, 193603 (2010).
- [23] D. Maxwell, D. J. Szwer, D. Paredes-Barato, H. Busche, J. D. Pritchard, A. Gauguet, K. J. Weatherill, M. P. A. Jones, and C. S. Adams, *Phys. Rev. Lett.* **110**, 103001 (2013).
- [24] O. Firstenberg, T. Peyronel, Q-Y. Liang, A. V. Gorshkov, M. D. Lukin and V. Vuletić *Nature* **502**, 71 (2013).
- [25] S. Baur, D. Tiarks, G. Rempe, and S. Dürr, *Phys. Rev. Lett.* **112**, 073901 (2014).
- [26] V. Parigi, E. Bimbard, J. Stanojevic, A. J. Hilliard, F. Nogrette, R. Tualle-Brouiri, A. Ourjoumtsev, and P. Grangier *Phys. Rev. Lett.* **109**, 233602 (2012).
- [27] H. Gorniaczyk, C. Tresp, J. Schmidt, H. Fedder, and S. Hofferberth *Phys. Rev. Lett.* **113**, 053601 (2014).
- [28] D. Tiarks, S. Baur, K. Schneider, S. Dürr, G. Rempe *Phys. Rev. Lett.* **113**, 053602 (2014).
- [29] Y. O. Dudin, and A. Kuzmich, *Science* **336**, 887 (2012).
- [30] A. Gaëtan, Y. Miroshnychenko, T. Wilk, A. Chotia, M. Viteau, D. Comparat, P. Pillet, A. Browaeys and P. Grangier *Nature. Phys* **5**, 115 (2009).
- [31] M. Müller, I. Lesanovsky, H. Weimer, H. P. Buchler, and P. Zoller, *Phys. Rev. Lett.* **102**, 170502 (2009).
- [32] L. Li, Y. O. Dudin, A. Kuzmich, *Nature* **498**, 466 (2013).
- [33] D. Paredes-Barato and C. S. Adams *Phys. Rev. Lett.* **112**, 040501 (2014).
- [34] M. Khazali, K. Heshami, C. Simon *Phys. Rev. A* **91**, 030301(R) (2015).
- [35] M. D. Lukin, M. Fleischhauer, R. Cote, L. M. Duan, D. Jaksch, J. I. Cirac, and P. Zoller *Phys. Rev. Lett.* **87**, 037901 (2001).
- [36] M. Saffman, T. G. Walker and K. Mølmer, *Rev. Mod. Phys.* **82**, 2313 (2010).
- [37] J. H. Shapiro, *Phys. Rev. A* **73**, 062305 (2006).
- [38] J. Gea-Banacloche, *Phys. Rev. A* **81**, 043823 (2010).
- [39] B. He and A. Scherer, *Phys. Rev. A* **85**, 033814 (2012); B. He, A.V. Sharypov, J. Sheng, C. Simon, and M. Xiao, *Phys. Rev. Lett.* **112**, 133606 (2014).
- [40] E. Bimbard, R. Boddeda, N. Vitrant, A. Grankin, V. Parigi, J. Stanojevic, A. Ourjoumtsev, and P. Grangier, *Phys. Rev. Lett.* **112**, 033601 (2014).
- [41] L. -M. Duan, H. J. Kimble, *Phys. Rev. Lett.* **92**, 127902 (2004).
- [42] A. V. Gorshkov, A. Andre, M. D. Lukin, A. S. Sørensen, *Phys. Rev. A* **76**, 033804 (2007).
- [43] See supplementary information for further details.
- [44] R. Löw, H. Weimer, J. Nipper, J. B. Balewski, B. Butscher, H. P. Büchler and T. Pfau, *J. Phys. B: At. Mol. Opt. Phys.* **45**, 113001 (2012).
- [45] J. Borregaard, P. Kómár, E. M. Kessler, M. D. Lukin, and A. S. Sørensen, *Phys. Rev. A* **92**, 012307 (2015).
- [46] N. Sangouard, C. Simon, B. Zhao, Y.-A. Chen, H. deRiedmaten, J.-W. Pan, and N. Gisin, *Phys. Rev. A* **77**, 062301 (2008).

Supplementary Material

THE REFLECTION COEFFICIENT

The dynamics of the Rydberg ensemble in the cavity can be described through the no-jump Hamiltonian \mathcal{H} consisting of the free energy and decay terms \mathcal{H}_s along with the interaction part as $\mathcal{H}_I = \mathcal{H}_{L\text{-int}} + \mathcal{H}_{\text{Ryd-int}}$, where

$$\begin{aligned}\mathcal{H}_s &= \sum_l \hbar(\Delta_l - i\Gamma_{el})|e_l\rangle\langle e_l| + \hbar(\delta_l - i\Gamma_{rl})|r_l\rangle\langle r_l| - i\hbar\kappa\hat{b}^\dagger\hat{b} \\ \mathcal{H}_{L\text{-int}} &= -\sum_l \frac{\hbar\Omega_l}{2}|r_l\rangle\langle e_l| - i\sum_l \hbar\mathcal{G}_l|e_l\rangle\langle g_l|\hat{b} + \text{H.c.} \\ \mathcal{H}_{\text{Ryd-int}} &= \sum_k \hbar\mathcal{V}_{kl}|r'_k\rangle\langle r'_k| \otimes |r_l\rangle\langle r_l|,\end{aligned}\tag{S9}$$

where the detunings Δ_l, δ_l , the linewidths Γ_e, Γ_r , and the coupling strengths Ω_l, \mathcal{G}_l are as defined in the main text, while 2κ is the cavity intensity decay rate. Note that all energies are measured relative to the cavity resonance, and hence the cavity term in \mathcal{H}_s only involve the loss rate κ . are as defined in the main text, while \mathcal{V}_{kl} is the van der Waals interaction among the Rydberg excitations of atoms k and l . The incoming and outgoing photons are going to be accounted for by the input-output relations. After the storage of the first pulse, the wave-function of the combined field and ensemble with the initial excitation stored in $|r'_k\rangle$ and one incoming photon is given by,

$$\begin{aligned}|\Psi\rangle &= \sum_k \int d\omega \beta_k(\omega) \hat{a}_\omega^\dagger e^{-i\omega t} |g^{N-1}, r'_k, \emptyset\rangle + \sum_k \hat{b}^\dagger C_{bk} |g^{N-1}, r'_k, \emptyset\rangle \\ &+ \sum_l \left\{ C_{ekl} |g^{N-2}, e_l, r'_k, \emptyset\rangle + C_{rkl} |g^{N-2}, r_l, r'_k, \emptyset\rangle \right\}.\end{aligned}\tag{S10}$$

Here $|\emptyset\rangle$ is the vacuum state, C_{ekl} and C_{rkl} are respectively the amplitude of being in the excited state $|e\rangle$ and the Rydberg state $|r\rangle$ when there is one stored Rydberg excitation in the k^{th} atom, while C_{bk} is the amplitude of the cavity excited state. We next evaluate the Schrödinger equation for the wave-function (S10) together with the input-output relations to find the dynamical behavior of the amplitudes C_{ak}, C_{ekl}, C_{rkl}

$$\dot{C}_{bk} = \sum_l C_{ekl} \mathcal{G}_l^* - \kappa C_{bk} + \sqrt{2\kappa} \beta_k^{\text{in}},\tag{S11}$$

$$\dot{C}_{ekl} = -i(\Delta_l - i\Gamma_{el})C_{ekl} + i\frac{\Omega_l^*}{2}C_{rkl} - \mathcal{G}_l C_{bk},\tag{S12}$$

$$\dot{C}_{rkl} = -i(\delta_l - i\Gamma_{rkl})C_{rkl} + i\frac{\Omega_l}{2}C_{ekl} - iC_{rkl}\mathcal{V}_{kl}.\tag{S13}$$

The outgoing field amplitude is then given by,

$$\beta_k^{\text{out}}(\omega) = \sqrt{2\kappa} C_{bk}(\omega) - \beta_k^{\text{in}}(\omega),\tag{S14}$$

where C_{bk} is found by solving the set of Eqns. (S11-S13) using Fourier transformation. We thereby get,

$$\begin{aligned}C_{bk}(\omega) &= \sqrt{2\kappa} \beta_k^{\text{in}}(\omega) \mathbf{S}_k(\omega) \\ \mathbf{S}_k(\omega) &= \left(\kappa - i\omega + \sum_l \frac{|\mathcal{G}_l|^2}{(\Gamma_{el} - i\Delta_l - i\omega) + \frac{|\Omega_l/2|^2}{\Gamma_{rl} + i(\delta_l + \mathcal{V}_{kl} - \omega)}} \right)^{-1}.\end{aligned}\tag{S15}$$

Substituting C_{bk} into Eq. (S14) we get,

$$\mathcal{R}_k(\omega) = 2\kappa \left(\kappa - i\omega + \sum_l \frac{|\mathcal{G}_l|^2}{(\Gamma_{el} - i\Delta_l - i\omega) + \frac{|\Omega_l/2|^2}{\Gamma_{rl} + i(\delta_l + \mathcal{V}_{kl} - \omega)}} \right)^{-1} - 1.\tag{S16}$$

Assuming all fields to be resonant i.e. for $\delta_l = \Delta_l = 0$, a long lived Rydberg state ($\Gamma_{rl} = 0$), and slowly varying photon pulses ($\omega = 0$) we get,

$$\mathcal{R}_k = 2 \left(1 + \sum_l \frac{|\mathcal{G}_l|^2 / \kappa \Gamma_e}{1 - i|\Omega_l/2|^2 / \mathcal{V}_{kl} \Gamma_e} \right)^{-1} - 1.\tag{S17}$$

which under the assumption of equal coupling strengths $\mathcal{G}_l = \mathcal{G}$ and Rabi frequencies $\Omega_l = \Omega$, for the defined single atom co-operativity $\mathcal{C} = |\mathcal{G}|^2/\kappa\Gamma_e$ becomes, $\mathcal{R}_k = \left[2(1 + \mathcal{C}_v^*)^{-1} - 1\right]$, where $\mathcal{C}_v^* = \sum_l \mathcal{C}/(1 - i|\Omega/2|^2/\mathcal{V}_{kl}\Gamma_e)$. To get a simple physical understanding of the scattering dynamics, we shall first assume that all atoms are identical (homogeneous). We will consider what happens for an inhomogeneous ensemble in a later section. For the van der Waals interaction potential $\mathcal{V}_{kl} = -C_6/r^6$, where r is the relative distance between the k^{th} and l^{th} atoms, we can evaluate \mathcal{C}_v^* with the sum \sum_l converted to a volume integral $\rightarrow \int ndV$. Thus we get for a homogeneous ensemble with an isotropic potential,

$$\mathcal{C}_v^* = 4\pi n\mathcal{C} \int_0^\infty dr r^2/(1 + i\zeta r^6); \zeta = \frac{|\Omega|^2}{4C_6\Gamma_e}. \quad (\text{S18})$$

We can write this integral as $\mathcal{C}_v^* = \mathcal{C}_b - i\mathcal{C}'_b$ and solved it to get, $|\mathcal{C}_b| = |\mathcal{C}'_b| = \frac{2}{3}(\mathcal{C}n\pi^2/\sqrt{2\zeta})$. Above, we have solved the scattering dynamics in the case where there was already a Rydberg excitation stored. In principle, we should also solve the dynamics without the first stored excitation. In this case, however, the excitations are completely independent of each other. We can then conveniently obtain the results for this situation by simple setting $\mathcal{V}_{kl} = 0$. Then from Eq. (S17) we get $\mathcal{C}_v^* = 0$ for a long photon pulse and hence $\mathcal{R}_g = 1$.

To investigate the effect of pulses of a finite duration, we now consider the bandwidth of the scattering coefficient. To do this, we perform a Taylor series expansion of the reflection coefficient about some central frequency ω_0 ,

$$\mathcal{R}_k(\omega) = \mathcal{R}_k(\omega_0) + \partial_\omega \mathcal{R}_k|_{\omega_0}(\omega - \omega_0) + \frac{1}{2}\partial_\omega^2 \mathcal{R}_k|_{\omega_0}(\omega - \omega_0)^2. \quad (\text{S19})$$

Here we have kept upto the second order in the expansion. The above three terms in the expansion are described by,

$$\mathcal{R}_k(\omega_0) = \left(\frac{2}{1 + \mathcal{C}_v^*} - 1\right) + 2i\frac{\omega_0}{\kappa} \frac{1}{(1 + \mathcal{C}_v^*)^2}, \quad (\text{S20})$$

$$\partial_\omega \mathcal{R}_k|_{\omega_0} = \frac{-4\frac{\omega_0}{\kappa} \left(\frac{1}{\kappa} - \frac{\mathcal{C}_{\alpha v}^*}{\Gamma_e}\right)}{(1 + \mathcal{C}_v^*)^3} + \frac{2i \left(\frac{1}{\kappa} - \frac{\mathcal{C}_{\alpha v}^*}{\Gamma_e}\right)}{(1 + \mathcal{C}_v^*)^2}, \quad (\text{S21})$$

$$\begin{aligned} \partial_\omega^2 \mathcal{R}_k|_{\omega_0} = & \frac{-4 \left(\frac{1}{\kappa} - \frac{\mathcal{C}_{\alpha v}^*}{\Gamma_e}\right)^2}{(1 + \mathcal{C}_v^*)^3} + \frac{4\mathcal{C}_v^* \frac{\mathcal{C}_{\beta v}^*}{\Gamma_e} \left[(\mathcal{C}_v^*)^2 - 3\frac{\omega_0^2}{\kappa^2}\right]}{(1 + \mathcal{C}_v^*)^6} + \frac{4\frac{\omega_0}{\kappa} \frac{\mathcal{C}_{\eta v}^*}{\Gamma_e^2}}{(1 + \mathcal{C}_v^*)^4} + \frac{4\frac{\mathcal{C}_{\chi v}^*}{\Gamma_e^2}}{(1 + \mathcal{C}_v^*)^3}, \\ -4i \left\{ & \frac{3\frac{\omega_0}{\kappa} \left(\frac{1}{\kappa} - \frac{\mathcal{C}_{\alpha v}^*}{\Gamma_e}\right)^2}{(1 + \mathcal{C}_v^*)^4} - \frac{\frac{\omega_0}{\kappa} \frac{\mathcal{C}_{\beta v}^*}{\Gamma_e^2} \left[3(\mathcal{C}_v^*)^2 - \frac{\omega_0^2}{\kappa^2}\right]}{(1 + \mathcal{C}_v^*)^6} + \frac{\frac{\mathcal{C}_{\eta v}^*}{\Gamma_e^2}}{(1 + \mathcal{C}_v^*)^3} + \frac{\frac{\omega_0}{\kappa} \frac{\mathcal{C}_{\chi v}^*}{\Gamma_e^2}}{(1 + \mathcal{C}_v^*)^4} \right\}, \end{aligned} \quad (\text{S22})$$

with the parameters defined by,

$$\mathcal{C}_v^* = \sum_l \frac{\mathcal{C}}{1 - i\frac{\omega_0}{\Gamma_e} + \frac{|\Omega_l/2|^2}{i(\mathcal{V}_{kl} - \omega_0)\Gamma_e}}, \quad \mathcal{C}_{\alpha v}^* = \mathcal{C} \sum_l \frac{1 + |\Omega_l/2|^2/(\mathcal{V}_{kl} - \omega_0)^2}{\left[1 - i\frac{\omega_0}{\Gamma_e} + \frac{|\Omega_l|^2}{i(\mathcal{V}_{kl} - \omega_0)\Gamma_e}\right]^2} \quad (\text{S23})$$

$$\mathcal{C}_{\beta v}^* = \mathcal{C} \sum_l \frac{1 + |\Omega_l/2|^2/(\mathcal{V}_{kl} - \omega_0)^2}{\left[1 - i\frac{\omega_0}{\Gamma_e} + \frac{|\Omega_l/2|^2}{i(\mathcal{V}_{kl} - \omega_0)\Gamma_e}\right]^3}, \quad \mathcal{C}_{\eta v}^* = \mathcal{C} \sum_l \frac{|\Omega_l/2|^2\Gamma_e/(\mathcal{V}_{kl} - \omega_0)^3}{\left[1 - i\frac{\omega_0}{\Gamma_e} + \frac{|\Omega_l/2|^2}{i(\mathcal{V}_{kl} - \omega_0)\Gamma_e}\right]^3} \quad (\text{S24})$$

$$\mathcal{C}_{\chi v}^* = \mathcal{C} \sum_l \frac{|\Omega_l/2|^2\omega_0/(\mathcal{V}_{kl} - \omega_0)^3}{\left[1 - i\frac{\omega_0}{\Gamma_e} + \frac{|\Omega_l/2|^2}{i(\mathcal{V}_{kl} - \omega_0)\Gamma_e}\right]^3}. \quad (\text{S25})$$

Assuming the central frequency of the incoming pulse to be on resonance, we set $\omega_0 = 0$ and hence Eqs. (S20-S22) become substantially simpler and are described by,

$$\mathcal{R}_k = \left(\frac{2}{1 + \mathcal{C}_v^*} - 1\right), \quad (\text{S26})$$

$$\partial_\omega \mathcal{R}_k|_{\omega_0=0} = \frac{2i \left(\frac{1}{\kappa} - \frac{\mathcal{C}_{\alpha v}^*}{\Gamma_e}\right)}{(1 + \mathcal{C}_v^*)^2}, \quad (\text{S27})$$

$$\partial_\omega^2 \mathcal{R}_k|_{\omega_0=0} = \frac{-4 \left(\frac{1}{\kappa} - \frac{\mathcal{C}_{\alpha v}^*}{\Gamma_e}\right)^2}{(1 + \mathcal{C}_v^*)^3} + \frac{4\mathcal{C}_v^* \frac{\mathcal{C}_{\beta v}^*}{\Gamma_e} (\mathcal{C}_v^*)^2}{(1 + \mathcal{C}_v^*)^6} + \frac{4\frac{\mathcal{C}_{\chi v}^*}{\Gamma_e^2}}{(1 + \mathcal{C}_v^*)^3} - 4i \left\{ \frac{\frac{\mathcal{C}_{\eta v}^*}{\Gamma_e^2}}{(1 + \mathcal{C}_v^*)^3} \right\}. \quad (\text{S28})$$

Note that for the case of no stored photon in the ensemble, we have $\mathcal{R}_k \rightarrow \mathcal{R}_g$ and one can also get the Taylor series expansion of \mathcal{R}_g by setting $\mathcal{V}_{kl} = 0$. The expressions for such an expansion at resonance is the same as given by Eqs. (S26 - S28) but now with the set of parameters, $\mathcal{C}_v^* \rightarrow \mathcal{C}^*$, $\mathcal{C}_{\alpha_v}^* \rightarrow \mathcal{C}_\alpha^*$, $\mathcal{C}_{\beta_v}^* \rightarrow \mathcal{C}_\beta^*$, $\mathcal{C}_{\eta_v}^* \rightarrow \mathcal{C}_\eta^*$, $\mathcal{C}_{\chi_v}^* \rightarrow \mathcal{C}_\chi^*$, where the new parameters correspond to Eqs. (S23 -S25) with $\mathcal{V}_{kl} = 0$. From the set of Eqs. (S26-S28), we see that the leading order dispersive contributions are scaled down by a factor of $(\mathcal{C}_v^*)^2$ and $(\mathcal{C}_v^*)^3$ when we compare the situation with and without stored excitation in the first pulse. Hence the spectrally narrowest feature is the width of the EIT resonance without a stored excitation, and this will thus be the limiting factor for the bandwidth.

We next analyze the behaviour of the parameters listed in Eqs. (S23-S25) in different limits of operation. We can find the blockaded part by considering the limits $\mathcal{V}_{kl} \gg |\Omega_l/2|^2/\Gamma_e$, while the contribution from the remaining EIT medium is found in the limit $\mathcal{V}_{kl} \ll |\Omega_l/2|^2/\Gamma_e$. To get a feeling for the expression in Eqs. (S23-S25), we separate them into contributions coming from the blockaded atoms and that from the rest of EIT medium,

$$\mathcal{C}_v^* \approx \mathcal{C}_b + i\mathcal{C}'_b = \sum_l \frac{\mathcal{C}}{\left[1 + \frac{|\Omega/2|^4}{\mathcal{V}_{kl}^2 \Gamma_e^2}\right]} + i \sum_l \frac{\mathcal{C} \frac{|\Omega/2|^2}{\mathcal{V}_{kl} \Gamma_e}}{\left[1 + \frac{|\Omega/2|^4}{\mathcal{V}_{kl} \Gamma_e^2}\right]}; \quad (\text{S29})$$

$$\mathcal{C}_{\alpha_v}^* = \mathcal{C}_b^{*\alpha} - N_{EIT}^\alpha \mathcal{C} \frac{\Gamma_e^2}{|\Omega/2|^2}, \quad \mathcal{C}_{\beta_v}^* = \mathcal{C}_b^{*\beta}; \quad (\text{S30})$$

$$\mathcal{C}_{\eta_v}^* = \mathcal{C}_b^{*\eta} - iN_{EIT}^\eta \mathcal{C} \frac{\Gamma_e^4}{|\Omega/2|^4}, \quad \mathcal{C}_{\chi_v}^* = 0, \quad (\text{S31})$$

where we have assumed all the Rabi frequencies to be equal such that $\Omega_l = \Omega$ and $\mathcal{C}_v^{*\alpha} = \sum_l \mathcal{C}/(1 + |\Omega/2|^2/i\mathcal{V}_{kl}\Gamma_e)^2$, $\mathcal{C}_v^{*\beta} = \mathcal{C}_v^{*\eta} = \sum_l \mathcal{C}/(1 + |\Omega/2|^2/i\mathcal{V}_{kl}\Gamma_e)^3$, which scale as the number of blocked atoms \mathcal{C}_b while $N_{EIT}^\alpha, N_{EIT}^\beta$ scale as the number of remaining unblocked atoms $\sim N$. Similarly, for the case of no stored excitation, we get,

$$\mathcal{C}^* = 0, \quad \mathcal{C}_\alpha^* = -N\mathcal{C} \frac{\Gamma_e^2}{|\Omega/2|^2}, \quad \mathcal{C}_\beta^* = 0; \quad (\text{S32})$$

$$\mathcal{C}_\eta^* = -iN\mathcal{C} \frac{\Gamma_e^4}{|\Omega/2|^4}, \quad \mathcal{C}_\chi^* = 0. \quad (\text{S33})$$

Note that since in this case there is no Rydberg excitation blockade, only the EIT medium contributes and all the terms arising due to blockade are zero.

CHOI-JAMIOLKOWSKI FIDELITY

The Choi-Jamiolkowski (CJ) fidelity is a measure of how close two given quantum mechanical processes are. The idea is to apply each process to a particular entangled state and then calculate the fidelity between the two output states. Specifically, we assume that the two processes are described by the superoperators \mathcal{U} and \mathcal{V} . The superoperator \mathcal{U} represents the ideal process that we want to accomplish and is assumed to be unitary. Hence, its action on some density matrix ρ can be written as

$$\mathcal{U}(\rho) = U\rho U^\dagger, \quad (\text{S34})$$

where U is a unitary operator. The actual physical implementation is represented by the completely positive trace preserving superoperator \mathcal{V} . In general, it admits a Kraus (operator-sum) decomposition

$$\mathcal{V}(\rho) = \sum_l V_l \rho V_l^\dagger \quad (\text{S35})$$

with $\sum_l V_l^\dagger V_l = I$ (I is the identity operator). If we separate out the ‘‘no jump’’ evolution with the effective non-Hermitian Hamiltonian \mathcal{H} in Eq. (S35), we can write

$$\mathcal{V}(\rho) = V\rho V^\dagger + \sum_l K_l \rho K_l^\dagger, \quad (\text{S36})$$

where $V = \exp(-i\mathcal{H}t_f/\hbar)$ with t_f being the time it takes to accomplish the wanted operation. The operators K_l form the Kraus decomposition of the part of the evolution where at least one quantum jump occurs.

To find the CJ fidelity, we consider the superoperators $\mathcal{I} \otimes \mathcal{U}$ and $\mathcal{I} \otimes \mathcal{V}$ that are tensor products of the original ones with the identity superoperator \mathcal{I} . We pick an orthonormal basis set $\{|j\rangle\}$ for the d -dimensional Hilbert space that \mathcal{U} and \mathcal{V} act on. Now

we can define the state $|\Phi\rangle = \sum_j |j\rangle|j\rangle/\sqrt{d}$ that is an element of the original Hilbert space tensored with a copy of itself. Note that $|\Phi\rangle$ is a maximally entangled state of these two copies. We will only consider a two-qubit gate, so that $d = 4$ in the above.

After applying $\mathcal{I} \otimes \mathcal{U}$ and $\mathcal{I} \otimes \mathcal{V}$ onto the density matrix $|\Phi\rangle\langle\Phi|$, we get a pair of new states

$$\rho_{\mathcal{U}} = [\mathcal{I} \otimes \mathcal{U}]|\Phi\rangle\langle\Phi| = (I \otimes U)|\Phi\rangle\langle\Phi|(I \otimes U^\dagger), \quad (\text{S37})$$

$$\rho_{\mathcal{V}} = [\mathcal{I} \otimes \mathcal{V}]|\Phi\rangle\langle\Phi| = (I \otimes V)|\Phi\rangle\langle\Phi|(I \otimes V^\dagger) + \sum_l (I \otimes K_l)|\Phi\rangle\langle\Phi|(I \otimes K_l^\dagger). \quad (\text{S38})$$

The CJ fidelity is defined to be the fidelity of these two states. Since $\rho_{\mathcal{U}}$ is a pure state, we get

$$\begin{aligned} F_{\text{CJ}} = F(\rho_{\mathcal{U}}, \rho_{\mathcal{V}}) &= \langle\Phi|(I \otimes U^\dagger)\rho_{\mathcal{V}}(I \otimes U)|\Phi\rangle \\ &= |\langle\Phi|(I \otimes U^\dagger V)|\Phi\rangle|^2 + \sum_l |\langle\Phi|(I \otimes U^\dagger K_l)|\Phi\rangle|^2. \end{aligned} \quad (\text{S39})$$

STORAGE AND RETRIEVAL

The full physical process to implement the controlled-phase gate consists of storage of one photon, scattering of the second one, and retrieval of the first. The theory of storage and retrieval with an ensemble in a cavity is well established. In suitable regimes these results show that we have a mapping between a single mode of the atomic ensemble and a specific incoming or outgoing optical mode, and all other modes will be uncoupled [1]. Hence, the process of storage is described by a single parameter, which is the storage efficiency of a single incoming photon to create a specific spin wave

$$|S\rangle = \sum_k \alpha_k |g^{N-1}, r'_k\rangle. \quad (\text{S40})$$

After scattering of the second photon, this spin wave will get multiplied by the reflection coefficient of the second photon such that it becomes

$$|S_{\mathcal{R}}\rangle = \sum_k \alpha_k \mathcal{R}_k(\omega) |g^{N-1}, r'_k\rangle,$$

where ω is the frequency of the second photon. Note here that the scattering coefficient may depend on which atom the first photon was stored in since different atoms may experience different degrees of blockade. For the retrieval, the cavity maps the particular spin wave (S40) to a specific temporal mode. Hence, the amplitude of the retrieved photon is given by the shape of that temporal mode multiplied by the overlap

$$\langle S|S_{\mathcal{R}}\rangle = \sum_k |\alpha_k|^2 \mathcal{R}_k(\omega).$$

In general, the retrieved wavepacket will also need to be multiplied by the square root of the overall storage and retrieval efficiency, but we neglect this in our analysis.

For the fidelity calculations, one would need to calculate the overlap of the retrieved photon wavepackets corresponding to $|S\rangle$ and $|S_{\mathcal{R}}\rangle$. However, by the discussion above, the overlap of the photon wavepackets will be equal to the overlap of the spin waves $|S\rangle$ and $|S_{\mathcal{R}}\rangle$. Hence, in the calculations below, we will directly calculate the fidelities by projecting the spin waves instead of analysing the retrieval.

FIDELITY IN THE SINGLE-RAIL ENCODING

In the single-rail encoding the computational basis is

$$\begin{aligned} |00(t)\rangle &= |g^N\rangle|\emptyset\rangle, \\ |01(t)\rangle &= |g^N\rangle \int d\omega \phi(\omega) \hat{a}_\omega^\dagger e^{-i\omega t} |\emptyset\rangle, \\ |10(t)\rangle &= \sum_k \alpha_k |g^{N-1}, r'_k\rangle |\emptyset\rangle, \\ |11(t)\rangle &= \sum_k \alpha_k |g^{N-1}, r'_k\rangle \int d\omega \phi(\omega) \hat{a}_\omega^\dagger e^{-i\omega t} |\emptyset\rangle. \end{aligned} \quad (\text{S41})$$

Note that this basis is time dependent due to the free evolution phase $\exp(-i\omega t)$. Hence, we define the ideal operation \mathcal{U} such that it includes this free evolution phase. Specifically, if we denote the computational basis states at the initial time $t = 0$ by omitting the time variable, i.e. $|jj'\rangle = |jj'(t=0)\rangle$ ($j, j' \in \{0, 1\}$), then the ideal operation of the controlled-phase gate is given by

$$U|00\rangle = |00(t_f)\rangle, \quad U|01\rangle = |01(t_f)\rangle, \quad U|10\rangle = |10(t_f)\rangle, \quad U|11\rangle = -|11(t_f)\rangle. \quad (\text{S42})$$

Using the computational basis (S41) we can write

$$|\Phi\rangle = \frac{1}{2} (|00\rangle|00\rangle + |01\rangle|01\rangle + |10\rangle|10\rangle + |11\rangle|11\rangle).$$

Inserting this specific form of $|\Phi\rangle$ into (S39) we obtain

$$F_{\text{CJ}} = \frac{1}{16} \left| \langle 00|U^\dagger V|00\rangle + \langle 01|U^\dagger V|01\rangle + \langle 10|U^\dagger V|10\rangle + \langle 11|U^\dagger V|11\rangle \right|^2 + \frac{1}{16} \sum_l \left| \langle 00|U^\dagger K_l|00\rangle + \langle 01|U^\dagger K_l|01\rangle + \langle 10|U^\dagger K_l|10\rangle + \langle 11|U^\dagger K_l|11\rangle \right|^2. \quad (\text{S43})$$

For the operators K_l , we assume that $\langle jj'(t_f)|K_l|jj'\rangle = 0$, where $j, j' \in \{0, 1\}$. Physically, this assumption means that if a quantum jump (incoherent decay) occurs, the given basis will switch to another state of the physical system (possibly even one of the other basis states) but can never be driven back to the original state. I.e. if a photon is lost, it will result in a vacuum output, and thus it does not give an overlap with the original state. Under this assumption, we only need to compute the dynamics due to the non-Hermitian Hamiltonian. The detailed calculation is presented in Sec. . In essence, the result is that the dynamics of the operator V can be described by the scattering relations

$$\begin{aligned} V|00\rangle &= |g^N\rangle|\emptyset\rangle, \\ V|01\rangle &= |g^N\rangle \int d\omega \mathcal{R}_g(\omega) \phi(\omega) \hat{a}_\omega^\dagger e^{-i\omega t_f} |\emptyset\rangle, \\ V|10\rangle &= \sum_k \alpha_k |g^{N-1}, r'_k\rangle |\emptyset\rangle, \\ V|11\rangle &= \int d\omega \sum_k \alpha_k \mathcal{R}_k(\omega) \phi(\omega) \hat{a}_\omega^\dagger e^{-i\omega t_f} |g^{N-1}, r'_k\rangle |\emptyset\rangle. \end{aligned} \quad (\text{S44})$$

Gathering all the formulas in this section, the CJ fidelity becomes

$$F_{\text{CJ}} = \frac{1}{16} \left| 2 + \int d\omega |\phi(\omega)|^2 \mathcal{R}_g(\omega) - \int d\omega |\phi(\omega)|^2 \sum_k |\alpha_k|^2 \mathcal{R}_k(\omega) \right|^2. \quad (\text{S45})$$

FIDELITY IN THE DUAL-RAIL ENCODING

In this section we calculate both the CJ fidelity and the entanglement swap fidelity for the dual-rail encoding and show how they relate to each other. The circuit diagram of the entanglement swap operation is shown in Fig. S4.

The entanglement swap operation consists of evolution of the initial state (which is unitary in the ideal case) and a subsequent measurement. The evolution can be decomposed into a controlled-phase gate and Hadamard gates. If the Hadamard gates are assumed to be ideal, then the CJ fidelity of the whole evolution is equal to the CJ fidelity of the controlled-phase gate. We are going to use this fact in relating the CJ fidelity to the entanglement swap fidelity.

The abstract definition of the CJ fidelity does not make any reference to a particular basis. In this section, in addition to the computational basis, we will also use the Bell basis, since it is the natural choice for the entanglement swap operation. The Bell states are

$$\begin{aligned} |\phi^{00}\rangle &= |\phi^+\rangle = \frac{1}{\sqrt{2}} (|00\rangle + |11\rangle), \\ |\phi^{01}\rangle &= |\psi^+\rangle = \frac{1}{\sqrt{2}} (|01\rangle + |10\rangle), \\ |\phi^{10}\rangle &= |\phi^-\rangle = \frac{1}{\sqrt{2}} (|00\rangle - |11\rangle), \\ |\phi^{11}\rangle &= |\psi^-\rangle = \frac{1}{\sqrt{2}} (|01\rangle - |10\rangle). \end{aligned} \quad (\text{S46})$$

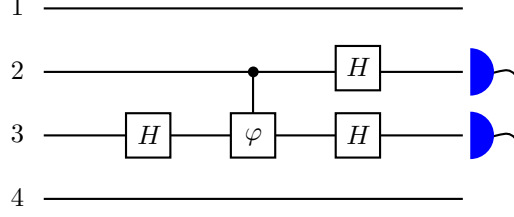


FIG. S4: (a) The circuit diagram of the entanglement swap operation. The numbers at the left edge indicate the label of the subsystem (qubit). In the circuit, the Hadamard gates are denoted by H and the controlled-phase gate is denoted by φ .

In addition to the conventional names, we also give numbers to the Bell states, which will allow us to express summations in a simple way below.

For the entanglement swap circuit of Fig. S4, the initial state is one Bell pair $|\phi^+\rangle_{12}$ between subsystems 1 and 2 and another Bell pair $|\phi^+\rangle_{34}$ between subsystems 3 and 4. Note that this initial state can be written as

$$|\phi^+\rangle_{12}|\phi^+\rangle_{34} = \frac{1}{2} \sum_{j,j'=0}^1 |\phi^{jj'}\rangle_{14}|\phi^{jj'}\rangle_{23} = |\Phi\rangle_{1423}.$$

This is exactly the state that is used as the input for the calculation of the CJ fidelity expressed in the Bell basis. After evolution of subsystems 2 and 3 as shown by the circuit and a measurement (the two detectors to the right), a Bell pair between subsystems 1 and 4 is established.

The practical implementation of the above circuit is shown in Fig. 1(c) of the main text. Whereas Fig. S4 displays the extended four-qubit Hilbert space required for the calculation of the CJ and entanglement swap fidelity, Fig. 1(c) only displays the two central subsystems (2 and 3), but each of the two subsystems are represented by the photon being in two distinct modes.

We define $\hat{a}_{0,\omega}^\dagger$ to be the creation operator for subsystem 3 in state $|0\rangle$ with frequency ω , and $\hat{a}_{1,\omega}^\dagger$ to be the creation operator for state $|1\rangle$. For notational convenience, we define the states $|0_\omega\rangle_3 = \hat{a}_{0,\omega}^\dagger|\emptyset\rangle$ and $|1_\omega\rangle_3 = \hat{a}_{1,\omega}^\dagger|\emptyset\rangle$. Then in the dual-rail encoding, the computational basis is

$$\begin{aligned} |0\rangle_2 &= \sum_k \alpha_k |g^{N-1}, r'_k\rangle_0, \\ |1\rangle_2 &= \sum_k \alpha_k |g^{N-1}, r'_k\rangle_1, \\ |0(t)\rangle_3 &= \int d\omega \phi(\omega) e^{-i\omega t} |0_\omega\rangle_3, \\ |1(t)\rangle_3 &= \int d\omega \phi(\omega) e^{-i\omega t} |1_\omega\rangle_3. \end{aligned} \tag{S47}$$

Here, $|g^{N-1}, r'_k\rangle_0$ are the states of the memory (the ensemble which does not interact with the second photon), and $|g^{N-1}, r'_k\rangle_1$ are the states of the cavity from which the second photon is scattered (see Fig. 1(c) of the main text). These two states correspond to subsystem 2 of Fig. S4. Subsystem 3 is encoded in photonic states which are not stored but only scattered. Note that all of the resulting computational basis states $|00\rangle_{23}$, $|01\rangle_{23}$, $|10\rangle_{23}$ and $|11\rangle_{23}$ physically correspond to having two excitations. Hence, it allows for simple means of error detection: if less than two excitations are present at the end of the evolution, we know that an error has occurred. In the dual-rail basis, the action of the operator V_{23} that corresponds to the physical implementation of the

controlled-phase gate can be written

$$\begin{aligned}
V_{23}|00\rangle_{23} &= \sum_k \alpha_k |g^{N-1}, r'_k\rangle_0 \int d\omega \phi(\omega) e^{-i\omega t_f} |0_\omega\rangle_3, \\
V_{23}|01\rangle_{23} &= \sum_k \alpha_k |g^{N-1}, r'_k\rangle_0 \int d\omega \mathcal{R}_g(\omega) \phi(\omega) e^{-i\omega t_f} |1_\omega\rangle_3, \\
V_{23}|10\rangle_{23} &= \sum_k \alpha_k |g^{N-1}, r'_k\rangle_1 \int d\omega \phi(\omega) e^{-i\omega t_f} |0_\omega\rangle_3, \\
V_{23}|11\rangle_{23} &= \int d\omega \sum_k \alpha_k \mathcal{R}_k(\omega) \phi(\omega) e^{-i\omega t_f} |g^{N-1}, r'_k\rangle_1 |1_\omega\rangle_3.
\end{aligned} \tag{S48}$$

For the operators corresponding to the full evolution of the circuit of Fig. S4, we also need to describe the Hadamard operators. In the dual-rail encoding, the Hadamard operations are obtained by impinging the photons on beamsplitters which work on all frequency components separately. This is important for subsystem 3 (the scattered photon), since the frequency components will be multiplied with, in general, different reflection coefficients $\mathcal{R}_g(\omega)$ and $\mathcal{R}_k(\omega)$ depending on the input state. Hence the definition of the Hadamard operator here needs to be per frequency component, i.e. $H_3|0_\omega\rangle_3 = (|0_\omega\rangle_3 + |1_\omega\rangle_3)/\sqrt{2}$ and $H_3|1_\omega\rangle_3 = (|0_\omega\rangle_3 - |1_\omega\rangle_3)/\sqrt{2}$. For subsystem 2, the single mode retrieval precludes any such difference in the mode shape for photons that are incident on the beamsplitters. Hence we can define the Hadamard operators to act on the spin wave states directly, $H_2|0\rangle_2 = (|0\rangle_2 + |1\rangle_2)/\sqrt{2}$ and $H_2|1\rangle_2 = (|0\rangle_2 - |1\rangle_2)/\sqrt{2}$.

In analogy with Eqs. (S34) and (S36), we define the superoperators \tilde{U} and \tilde{V} for the ideal and the real version of the circuit of Fig. S4. They can be written as

$$\tilde{U}_{23}(\rho) = \tilde{U}_{23} \rho \tilde{U}_{23}^\dagger,$$

and

$$\tilde{V}_{23}(\rho) = \tilde{V}_{23} \rho \tilde{V}_{23}^\dagger + \sum_l \tilde{K}_{l,23} \rho \tilde{K}_{l,23}^\dagger,$$

where

$$\begin{aligned}
\tilde{U}_{23} &= (H_2 \otimes H_3) U_{23} (I_2 \otimes H_3), \\
\tilde{V}_{23} &= (H_2 \otimes H_3) V_{23} (I_2 \otimes H_3), \\
\tilde{K}_{l,23} &= (H_2 \otimes H_3) K_{l,23} (I_2 \otimes H_3).
\end{aligned} \tag{S49}$$

Note that with the definitions (S42), (S46) and (S49), it holds that $\tilde{U}_{23}|\phi^{jj'}\rangle = |jj'(t_f)\rangle$.

In this setting, not only the input states used for the entanglement swapping match the ones used for the CJ fidelity, also the actual operation itself has the same form: an identity operation acting on subsystems 1 and 4, while subsystems 2 and 3 are evolved according to either \tilde{U} or \tilde{V} . The two output states are then

$$\begin{aligned}
\rho_{\tilde{U}} &= [\mathcal{I}_{14} \otimes \tilde{U}_{23}] (|\Phi\rangle\langle\Phi|) = (I_{14} \otimes \tilde{U}_{23}) |\Phi\rangle\langle\Phi| (I_{14} \otimes \tilde{U}_{23}^\dagger), \\
\rho_{\tilde{V}} &= [\mathcal{I}_{14} \otimes \tilde{V}_{23}] (|\Phi\rangle\langle\Phi|) = (I_{14} \otimes \tilde{V}_{23}) |\Phi\rangle\langle\Phi| (I_{14} \otimes \tilde{V}_{23}^\dagger) + \sum_l (I_{14} \otimes \tilde{K}_{l,23}) |\Phi\rangle\langle\Phi| (I_{14} \otimes \tilde{K}_{l,23}^\dagger).
\end{aligned}$$

Now we want to use the error detection property of the dual-rail encoding. We define the projection operators

$$\hat{P}_{jj'} = I_{14} \otimes |j\rangle\langle j|_2 \otimes \left(\int d\omega |j'_\omega\rangle\langle j'_\omega|_3 \right) \tag{S50}$$

where $j, j' \in \{0, 1\}$, and we also define their sum

$$\hat{P} = \sum_{j,j'=0}^1 \hat{P}_{jj'}. \tag{S51}$$

The projection operators of Eq. (S50) correspond to measuring the states $|jj'\rangle_{23}$ on the detectors of circuit of Fig. S4. Note that for subsystem 3, we project onto the entire subspace that is spanned by the states $|j'_\omega\rangle$ instead of choosing a particular mode. This is equivalent to the assumption that all frequency components contribute to the probability of a ‘‘click’’ on the detector. On the

other hand, the operator of Eq. (S51) has a less clear physical interpretation. Formally, it projects a given state onto the subspace with two excitations. The motivation for defining such an operator is to be able to relate the CJ fidelity to the entanglement swap fidelity as we will see below. Since the entanglement swap fidelity can only be understood as a conditional fidelity (conditioned on the measurement outcomes corresponding to the operators of Eq. (S50)), the CJ fidelity also needs to be conditional.

Let us begin with the calculation of the entanglement swap fidelity. Using the states after the measurement has taken place

$$\rho_{jj'} = \frac{\hat{P}_{jj'} \rho_{\tilde{V}} \hat{P}_{jj'}^\dagger}{\text{tr}(\hat{P}_{jj'} \rho_{\tilde{V}} \hat{P}_{jj'}^\dagger)},$$

we can define the conditional fidelities for the entanglement swap

$$F_{jj'} = \langle \phi^{jj'} | \text{tr}_{23}(\rho_{jj'}) | \phi^{jj'} \rangle_{14}. \quad (\text{S52})$$

Here, we take the trace over subsystems 2 and 3, since the relevant question is how close subsystems 1 and 4 are to a particular Bell pair. The trace can be written as

$$\text{tr}_{23}(\rho_{jj'}) = \sum_{n,n'=0}^1 \int d\omega \langle n | {}_2 \langle n'_\omega | {}_3 \rho_{jj'} | n'_\omega \rangle_3 | n \rangle_2 = \frac{1}{\text{tr}(\hat{P}_{jj'} \rho_{\tilde{V}} \hat{P}_{jj'}^\dagger)} \int d\omega \langle j | {}_2 \langle j'_\omega | {}_3 \rho_{\tilde{V}} | j'_\omega \rangle_3 | j \rangle_2.$$

Projecting $\rho_{\tilde{V}}$ onto $|\phi^{jj'}\rangle_{14}$ we obtain

$$\langle \phi^{jj'} | \rho_{\tilde{V}} | \phi^{jj'} \rangle_{14} = \frac{1}{4} \tilde{V}_{23} |\phi^{jj'}\rangle_{23} \langle \phi^{jj'} | {}_{23} \tilde{V}_{23}^\dagger + \frac{1}{4} \sum_l \tilde{K}_{l,23} |\phi^{jj'}\rangle_{23} \langle \phi^{jj'} | {}_{23} \tilde{K}_{l,23}^\dagger.$$

For the dual-rail encoding, we have a stronger assumption about the operators K_l than for the single-rail encoding. We are going to assume that $\langle n | {}_2 \langle n'_\omega | {}_3 K_l | j j' \rangle = 0$, where $n, n', j, j' \in \{0, 1\}$. Physically, this assumption means that the decay processes take the state out of the computational basis entirely, since any such decay will reduce the number of the total excitations to less than two. Then the expression for the fidelity (S52) becomes

$$F_{jj'} = \frac{1}{4 \text{tr}(\hat{P}_{jj'} \rho_{\tilde{V}} \hat{P}_{jj'}^\dagger)} \int d\omega \left| \langle j | {}_2 \langle j'_\omega | {}_3 (H_2 \otimes H_3) V_{23} (I_2 \otimes H_3) | \phi^{jj'} \rangle_{23} \right|^2.$$

with the trace in the denominator given by

$$\text{tr}(\hat{P}_{jj'} \rho_{\tilde{V}} \hat{P}_{jj'}^\dagger) = \frac{1}{4} \sum_{n,n'=0}^1 \int d\omega \left| \langle n | {}_2 \langle n'_\omega | {}_3 (H_2 \otimes H_3) V_{23} (I_2 \otimes H_3) | \phi^{jj'} \rangle_{23} \right|^2.$$

For all j and j' we get

$$\text{tr}(\hat{P}_{jj'} \rho_{\tilde{V}} \hat{P}_{jj'}^\dagger) = \frac{1}{16} \int d\omega |\phi(\omega)|^2 \left(2 + |\mathcal{R}_g(\omega)|^2 + \left| \sum_k |\alpha_k|^2 \mathcal{R}_k(\omega) \right|^2 \right)$$

and

$$F_{\text{swap}} = F_{jj'} = \frac{1}{16 P_{\text{suc}}} \int d\omega |\phi(\omega)|^2 \left| 2 + \mathcal{R}_g(\omega) - \sum_k |\alpha_k|^2 \mathcal{R}_k(\omega) \right|^2, \quad (\text{S53})$$

where we have defined the success probability $P_{\text{suc}} = \sum_{j,j'=0}^1 \text{tr}(\hat{P}_{jj'} \rho_{\tilde{V}} \hat{P}_{jj'}^\dagger)$, i.e.

$$P_{\text{suc}} = \frac{1}{4} \int d\omega |\phi(\omega)|^2 \left(2 + |\mathcal{R}_g(\omega)|^2 + \left| \sum_k |\alpha_k|^2 \mathcal{R}_k(\omega) \right|^2 \right). \quad (\text{S54})$$

Now we look at the conditional CJ fidelity. Using the state

$$\rho'_{\tilde{V}} = \frac{\hat{P} \rho_{\tilde{V}} \hat{P}^\dagger}{\text{tr}(\hat{P} \rho_{\tilde{V}} \hat{P}^\dagger)} \quad (\text{S55})$$

we can define the conditional CJ fidelity as $F'_{\text{CJ}} = F(\rho'_{\tilde{U}}, \rho'_{\tilde{V}})$. By the cyclicity and linearity of the trace, we have

$$\text{tr}(\hat{P}\rho_{\tilde{V}}\hat{P}^\dagger) = \sum_{j,j'=0}^1 \text{tr}(\hat{P}_{jj'}\rho_{\tilde{V}}\hat{P}_{jj'}^\dagger) = P_{\text{suc}}.$$

The projection operator \hat{P} has no effect on the states $|\Phi\rangle$, hence $F(\rho_{\tilde{U}}, \hat{P}\rho_{\tilde{V}}\hat{P}^\dagger) = F(\rho_{\tilde{U}}, \rho_{\tilde{V}})$, and the analysis reduces to finding the unconditional CJ fidelity and dividing by the success probability P_{suc} . The final result is

$$F'_{\text{CJ}} = \frac{1}{16P_{\text{suc}}} \left| 2 + \int d\omega |\phi(\omega)|^2 \mathcal{R}_g(\omega) - \int d\omega |\phi(\omega)|^2 \sum_k |\alpha_k|^2 \mathcal{R}_k(\omega) \right|^2. \quad (\text{S56})$$

Comparing Eqs. (S53) and (S56) we see that the only difference is the order of integration and taking the absolute value. Thus in general, we have $F'_{\text{CJ}} \leq F_{\text{swap}}$. If the bandwidth of the second photon is narrow compared to the the frequency variations of \mathcal{R}_g and \mathcal{R}_k , then the two fidelity measures become equal. The reason for this similarity is that the two measures consider the same input, but they do not consider exactly the same output. For the CJ fidelity the question we ask is what is the output with a particular mode, which we for simplicity take to be the same as the input mode. Possibly the CJ fidelity can therefore be increased by considering a more appropriate output mode. For the swapping fidelity we on the other hand consider everything which is incident on the photodetectors regardless of the temporal mode and hence this fidelity is higher.

THE GATE FIDELITIES FOR THE RYDBERG CONTROLLED-PHASE GATE

In the single-rail case, we evaluate the CJ fidelity (S45). To evaluate the quantity inside the modulus square we expand it and use Eq. (S19) and the corresponding expansion for \mathcal{R}_g to get,

$$\Delta\mathcal{R} = \mathcal{R}_g - \sum_k |\alpha_k|^2 \mathcal{R}_k = \frac{2\mathcal{C}_b + 2i\mathcal{C}'_b}{(1 + \mathcal{C}_b) + i\mathcal{C}'_b} \quad (\text{S57})$$

$$\Delta\mathcal{R}' = \left[\mathcal{R}'_g - \sum_k |\alpha_k|^2 \mathcal{R}'_k \right] = 2i \left(\frac{1}{\kappa} + \frac{N\mathcal{C}\Gamma_e}{|\Omega/2|^2} \right) - 2i \left(\frac{1}{\kappa} + \frac{N_{\text{EIT}}^\alpha \mathcal{C}\Gamma_e}{|\Omega/2|^2} \right) \frac{1}{(1 + \mathcal{C}_b)^2} + \frac{2i\mathcal{C}_b^{*\alpha}}{\Gamma_e} \quad (\text{S58})$$

$$\begin{aligned} \Delta\mathcal{R}'' &= \left[\mathcal{R}''_g - \sum_k |\alpha_k|^2 \mathcal{R}''_k \right] = -4 \left(\frac{1}{\kappa} + \frac{N\mathcal{C}\Gamma_e}{|\Omega/2|^2} \right)^2 + 4 \left(\frac{1}{\kappa} + \frac{N_{\text{EIT}}^\alpha \mathcal{C}\Gamma_e}{|\Omega/2|^2} \right)^2 \frac{1}{(1 + \mathcal{C}_b)^3} \\ &+ 4 \frac{(\frac{\mathcal{C}_b^{*\alpha}}{\Gamma_e})^2}{(1 + \mathcal{C}_b)^3} - 4 \frac{N\Gamma_e^2 \mathcal{C}}{|\Omega/2|^4} + 4 \frac{N_{\text{EIT}}^\eta \Gamma_e^2 \mathcal{C}}{|\Omega/2|^4} \frac{1}{(1 + \mathcal{C}_b)^3} - 4 \frac{\mathcal{C}_b^{*\beta}}{\mathcal{C}_b^3} + 4i \frac{\mathcal{C}_b^{*\eta}}{\Gamma_e^2 (1 + \mathcal{C}_b)^3} \end{aligned} \quad (\text{S59})$$

In deriving the above expressions, we have assumed that the ensemble is homogeneous and that the potential is isotropic. Hence we have dropped the index k from \mathcal{V}_{kl} . We can then do the sum over k and given that α_k are normalized, we have $\sum_k |\alpha_k|^2 = 1$ in the above expressions.

A closer look at Eq. (S45) suggests a further simplification which gives us,

$$F_{\text{CJ}} = \frac{1}{16} \left(4 + |\Delta\mathcal{R}|^2 + 4\mathbf{Re}[\Delta\mathcal{R}] + 2\mathbf{Re}[\Delta\mathcal{R}''](\Delta\omega)^2 + \mathbf{Re}[\Delta\mathcal{R}\Delta\mathcal{R}''^*](\Delta\omega)^2 \right) \quad (\text{S60})$$

where we have assumed narrow bandwidth of the pulse and defined the variance of the incoming pulse as $(\Delta\omega)^2 = \int d\omega |\phi(\omega)|^2 (\omega - \omega_0)^2$. Substituting Eqs. (S57 - S59) in Eq. (S60) and assuming that $\mathcal{C}_b, \mathcal{C}'_b \gg 1$ and $\mathcal{C}_b^{*\beta}, \mathcal{C}_b^{*\alpha} < \mathcal{C}_b^2$, we get,

$$\begin{aligned} F_{\text{CJ}} &\simeq \left[1 - \frac{(1 + \mathcal{C}_b)}{(1 + \mathcal{C}_b)^2 + \mathcal{C}_b'^2} \right] + \frac{1}{4[(1 + \mathcal{C}_b)^2 + \mathcal{C}_b'^2]} - \frac{N\mathcal{C}\Gamma_e^2}{2|\Omega/2|^4} (\Delta\omega)^2 \left(1 + \frac{\mathcal{C}_b(1 + \mathcal{C}_b) + \mathcal{C}_b'^2}{(1 + \mathcal{C}_b)^2 + \mathcal{C}_b'^2} \right) \\ &- \frac{1}{2} \left(\frac{1}{\kappa} + \frac{N\mathcal{C}\Gamma_e}{|\Omega/2|^2} \right)^2 \left(1 + \frac{\mathcal{C}_b(1 + \mathcal{C}_b) + \mathcal{C}_b'^2}{(1 + \mathcal{C}_b)^2 + \mathcal{C}_b'^2} \right) (\Delta\omega)^2 \end{aligned} \quad (\text{S61})$$

Considering only the leading order contribution to the fidelity, we get,

$$F_{\text{CJ}} = 1 - \frac{(1 + C_b)}{(1 + C_b)^2 + C_b'^2} - \frac{N\mathcal{C}\Gamma_e^2}{|\Omega/2|^4}(\Delta\omega)^2 - \left(\frac{1}{\kappa} + \frac{N\mathcal{C}\Gamma_e}{|\Omega/2|^2}\right)^2 (\Delta\omega)^2 \quad (\text{S62})$$

For the dual-rail case, we calculate a conditional swap fidelity (S53) and the success probability (S54). We can write (S53) as

$$F_{\text{swap}} = \frac{1}{16P_{\text{suc}}} \left(4 + |\Delta\mathcal{R}|^2 + 4\text{Re}[\Delta\mathcal{R}] + |\Delta\mathcal{R}'|^2(\Delta\omega)^2 + 2\text{Re}[\Delta\mathcal{R}''](\Delta\omega)^2 + \text{Re}[\Delta\mathcal{R}\Delta\mathcal{R}''^*](\Delta\omega)^2 \right) \quad (\text{S63})$$

which under the assumption that $C_b, C_b' \gg 1$ and $C_b^{*\beta}, C_b^{*\alpha} < C_b^2$, becomes,

$$\begin{aligned} &= \frac{1}{16P_{\text{suc}}} \left(16 \left[1 - \frac{(1 + C_b)}{(1 + C_b)^2 + C_b'^2} \right] + \frac{4}{(1 + C_b)^2 + C_b'^2} - \frac{8N\mathcal{C}\Gamma_e^2}{|\Omega/2|^4}(\Delta\omega)^2 \left(1 + \frac{C_b(1 + C_b) + C_b'^2}{(1 + C_b)^2 + C_b'^2} \right) \right. \\ &- 8 \left(\frac{1}{\kappa} + \frac{N\mathcal{C}\Gamma_e}{|\Omega/2|^2} \right)^2 \left(1 + \frac{C_b(1 + C_b) + C_b'^2}{(1 + C_b)^2 + C_b'^2} \right) (\Delta\omega)^2 + 4 \left(\frac{1}{\kappa} + \frac{N\mathcal{C}\Gamma_e}{|\Omega/2|^2} \right)^2 (\Delta\omega)^2 \\ &\left. - 8 \left(\frac{1}{\kappa} + \frac{N\mathcal{C}\Gamma_e}{|\Omega/2|^2} \right) \left(\frac{1}{\kappa} + \frac{N_{\text{EIT}}^\alpha \mathcal{C}\Gamma_e}{|\Omega/2|^2} \right) \frac{1}{(1 + C_b)^2} (\Delta\omega)^2 \right) \quad (\text{S64}) \end{aligned}$$

The success probability (S54) is then

$$P_{\text{suc}} = \frac{1}{4} \left(2 + |\mathcal{R}_g|^2 + |\mathcal{R}_g'|^2(\Delta\omega)^2 + \text{Re}[\mathcal{R}_g\mathcal{R}_g''^*](\Delta\omega)^2 + |\mathcal{R}_k|^2 + |\mathcal{R}_k'|^2(\Delta\omega)^2 + \text{Re}[\mathcal{R}_k\mathcal{R}_k''^*](\Delta\omega)^2 \right), \quad (\text{S65})$$

which under the assumption that $C_b, C_b' \gg 1$ and $C_b^{*\beta}, C_b^{*\alpha} < C_b^2$, becomes,

$$P_{\text{suc}} = 1 - \frac{C_b}{(1 + C_b)^2 + C_b'^2} - \frac{N\mathcal{C}\Gamma_e^2}{|\Omega/2|^4}(\Delta\omega)^2 \quad (\text{S66})$$

Substituting Eq. (S66) and (S61) into Eq. (S53), we get the expression for the conditional swap fidelity,

$$F_{\text{swap}} \simeq 1 - \frac{3}{4[C_b^2 + C_b'^2 + 2C_b]} - \frac{C_b^2}{[C_b^2 + C_b'^2 + 2C_b]^2} - \frac{3}{4} \left[\frac{1}{\kappa} + \frac{N\mathcal{C}\Gamma_e}{|\Omega/2|^2} \right]^2 \left[1 + \frac{C_b}{C_b^2 + C_b'^2 + 2C_b} \right] (\Delta\omega)^2 \quad (\text{S67})$$

Finally, keeping only the dominant contribution to the gate operation, we get the conditional swap fidelity,

$$F_{\text{swap}} = 1 - \frac{1}{[C_b^2 + C_b'^2]} - \frac{3C_b^2 - C_b'^2}{4[C_b^2 + C_b'^2]^2} - \frac{3}{4} \left[\frac{1}{\kappa} + \frac{N\mathcal{C}\Gamma_e}{|\Omega/2|^2} \right]^2 (\Delta\omega)^2 \quad (\text{S68})$$

INHOMOGENEOUS ENSEMBLE

So far, we have considered only a homogeneous ensemble without decay of the Rydberg level. In this section we discuss the case for an inhomogeneous ensemble. For simplicity, we only consider $\Delta\omega = 0$. Here the scattering dynamics depends on where the excitation was stored in the ensemble. From the fidelity expressions Eq. (S45) and Eq. (S53) we see that the essential parameter is $\sum_k |\alpha_k|^2 \mathcal{R}_k$ which for $\delta_l = \Delta_l = 0$ is given by

$$\sum_k |\alpha_k|^2 \mathcal{R}_k = \sum_k |\alpha_k|^2 \left[\frac{2}{1 + \sum_l \frac{|\mathcal{G}_l|^2 / \kappa \Gamma_{el}}{1 + |\Omega_l/2|^2 / (\Gamma_{rl} \Gamma_{el} + i\mathcal{V}_{kl} \Gamma_{el})}} - 1 \right]. \quad (\text{S69})$$

When the ensemble was homogeneous, we defined the blockaded co-operativity C_b and C_b' such that $\mathcal{R}_k = \frac{1}{1 + C_b + iC_b'}$. Analogous to this for an inhomogeneous ensemble, we can define the blockaded co-operativity through $\sum_k |\alpha_k|^2 \mathcal{R}_k = 1/(1 + C_b^{\text{inh}} + iC_b'^{\text{inh}})$

where,

$$\begin{aligned} \mathcal{C}_b^{\text{inh}} &= \mathbf{Re} \left[\frac{1}{\sum_k |\alpha_k|^2 \left(1 + \sum_{l \neq k} \frac{\mathcal{C}_l}{1 + |\Omega/2|^2 / (\Gamma_{rl} \Gamma_{el} + i \mathcal{V}_{kl} \Gamma_{el})} \right)^{-1}} \right] - 1, \\ \mathcal{C}'_b{}^{\text{inh}} &= \mathbf{Im} \left[\frac{1}{\sum_k |\alpha_k|^2 \left(1 + \sum_{l \neq k} \frac{\mathcal{C}_l}{1 + |\Omega/2|^2 / (\Gamma_{rl} \Gamma_{el} + i \mathcal{V}_{kl} \Gamma_{el})} \right)^{-1}} \right] \end{aligned} \quad (\text{S70})$$

Note that contrary to the homogeneous case the above defined effective co-operativity for inhomogeneous ensemble also includes the effect of Rydberg decoherence on the scattering process. Thus, to study the Fidelity of the phase gate for an inhomogeneous ensemble and in presence of decoherence, the results in Eqs. (S62) and (S68) can be utilized but now with \mathcal{C}_b replaced by $\mathcal{C}_b^{\text{inh}}$ and \mathcal{C}'_b by $\mathcal{C}'_b{}^{\text{inh}}$.

* Electronic address: sumanta@nbi.ku.dk

† Electronic address: andrey.grankin@u-psud.fr

[1] Alexey V. Gorshkov, Axel André, Mikhail D. Lukin, Anders S. Sørensen, Phys. Rev. A **76**, 033804 (2007)